Provided for non-commercial research and education use.
Not for reproduction, distribution or commercial use.

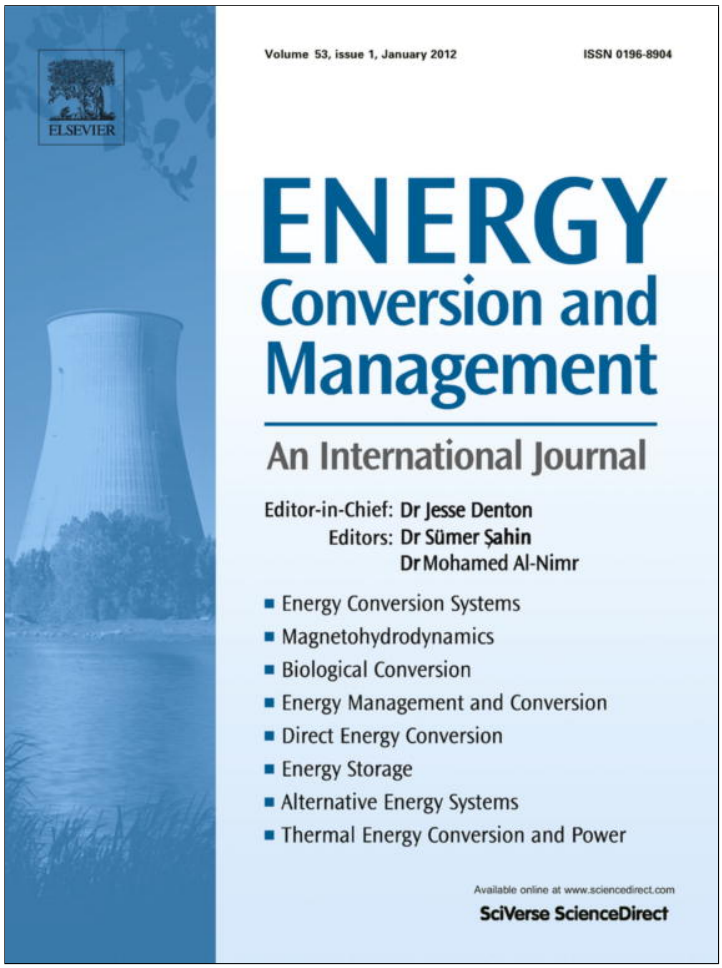

(This is a sample cover image for this issue. The actual cover is not yet available at this time.)

This article appeared in a journal published by Elsevier. The attached copy is furnished to the author for internal non-commercial research and education use, including for instruction at the authors institution and sharing with colleagues.

Other uses, including reproduction and distribution, or selling or licensing copies, or posting to personal, institutional or third party websites are prohibited.

In most cases authors are permitted to post their version of the article (e.g. in Word or Tex form) to their personal website or institutional repository. Authors requiring further information regarding Elsevier's archiving and manuscript policies are encouraged to visit:

http://www.elsevier.com/copyright

Author's personal copy

Energy Conversion and Management 68 (2013) 96–104

Contents lists available at SciVerse ScienceDirect

Energy Conversion and Management

journal homepage: www.elsevier.com/locate/enconman

Optimization strategies to reduce the biodiesel NOx effect in diesel engine with experimental verification

Mohamed F. Al-Dawody *, S.K. Bhatti

Department of Mechanical Engineering, Andhra University, Visakhapatnam, 530 003 AP, India

ARTICLE INFO

Article history:
Received 23 November 2012
Received in revised form 30 December 2012
Accepted 31 December 2012

Keywords:
Multi-zone
Diesel engine
Performance
Emissions
Biodiesel
NOx
Optimization

ABSTRACT

In this study the combustion, performance and emission parameters of single cylinder, four stroke, constant speed diesel engine operating on diesel oil and different blends of soybean methyl ester (SME) have been investigated experimentally and also theoretically using the simulation software Diesel-rk. It was found that 25.27%, 36.93%, and 52.96% reduction in the Bosch smoke number is obtained with B20% SME, B40% SME and B100% SME respectively, as compared to pure diesel fuel. All blends of biodiesel are observed to emit higher NOx emissions relative to that of nominal diesel level. The results point out that B20% SME was the best one which gives little performance differences with good reduction in emissions when compared to diesel fuel. Different strategies are adopted to control biodiesel NOx effect on the B20% SME. From the one dimensional strategy it is observed that cooling air temperature from (55 to 15) °C reduce NOx, air pollutant emissions (SE), Bosch smoke number and brake specific fuel consumption (BSFC) by 10.53%, 17.63%, 24.35%, and 6.2% respectively with respect to base line operation. Deeper piston bowel with small diameter gives a significant reduction in the NOx emissions. According to scanning 2-dimensional strategy it is found that the best reduction in the NOx, air pollutant emissions and Bosch smoke number is 22.84%, 20.2%, and 8.31% respectively while BSFC is increased by 5.14% at 19 compression ratio and 0.06 exhaust gas recirculation ratio (EGR). A multiparametric optimization technique using Rosenbrok method for diesel engine operating on B20% SME was investigated theoretically. The optimization gives 50.26% reduction in NOx emissions. The theoretical simulation results are verified with the experimental study conducted at the same operating conditions.

© 2013 Elsevier Ltd. All rights reserved.

1. Introduction

In recent years, the fossil-fuels have suffered from a sudden rise in prices because of the limitations of deposit, supply and considerable increase in demand for petroleum fuels resulting from the industrialization. Furthermore, the regulations for particulate matter (PM) and NOx emissions from diesel engines have strengthened, and reductions in carbon dioxide (CO_2), which is a greenhouse gas, emissions also raised important issues on environmental problems [1,2]. For these reasons, biodiesel has been subjected to intensive research work all over the world. Biodiesel is a non-toxic, biodegradable and renewable alternative fuel that can be used with no engine modifications. It can be produced from various vegetable oils, waste cooking oils and animal fats. The fuel properties of biodiesel may change when different feed stocks are used. In general, if the fuel properties of biodiesel are compared to petroleum diesel fuel, it can be seen that biodiesel has higher viscosity, density, and cetane number, but the energy content or net calorific value of biodiesel is about 10–12% less than that of conventional diesel fuel [3]. In the last three decades, the impact of biodiesel produced from different feed stocks has been intensively investigated on the performance and emission characteristic of diesel engine by many researchers. These studies point out that biodiesel exhibits similar results with very little performance differences and reductions on regulated emissions when compared to nominal diesel operation. Therefore, it may not require modifications on diesel engines to use biodiesel. There is a general agreement on the biodiesel which provides substantial reduction in hydrocarbon (HC), carbon monoxide (CO), and smoke emissions but it increases the NOx emissions compared to pure diesel fuel. Soybean is a very versatile grain that gives rise to products widely used by agro-chemical industry and food industry. Besides this it is a raw material for extraction of oil for biofuel production. Soybean has about 25% of oil content in grain. The largest producers of soybeans are: United States, Brazil, Argentina, China and India [4]. Many researchers have found that although biodiesel fuels could reduce PM, CO and smoke exhaust emissions, NOx emissions were increased compared to petroleum based diesel fuel in diesel engines [5–21]. The cause of this increase is not fully known, but it has been largely attributed to differences in the physical properties

* Corresponding author. Tel.: +91 08912500718.
E-mail addresses: rukia612010@gmail.com (M.F. Al-Dawody), sukhvinder_bhatti@yahoo.com (S.K. Bhatti).

0196-8904/$ - see front matter © 2013 Elsevier Ltd. All rights reserved.
http://dx.doi.org/10.1016/j.enconman.2012.12.025

Author's personal copy

Nomenclature

Symbol	Definition and unit
A_o, A_2, A_3	constants
B20	blend containing 80% of diesel oil and 20% SME by volume
B40	blend containing 60% of diesel oil and 40% SME by volume
B100	blend containing 100% SME by volume
BMEP	brake mean effective pressure (bar)
BSFC	brake specific fuel consumption (g/kW h)
BSN	Bosch smoke number
BTDC	before top dead center
[C]	soot concentration in the cylinder
°C	degree centigrade
°CA	crank angle degree
CN	cetane number of fuel
C_{PM}	empirical factor for PM emission
C_{NO}	empirical factor for NOx emission
CO	carbon monoxide
E_a	apparent activation energy for the auto ignition process 23,000–28,000 kJ/kmole
EFM	elementary fuel mass
K_T	evaporation constant
l	current length of the spray (m)
lm	penetration distance of the control portion of fuel (m)
m_f	mass of fuel
NOx	nitrogen oxides (ppm)
p	pressure in the cylinder (Pa)
ps	saturation pressure of the fuel vapor (Pa)
PM	particulate matter
R	universal gas constant (8.3143 kJ/kmol °K)
rpm	revolution per minute
rps	revolution per second
SE	summary of (PM & NOx emissions) (g/kW h)
SME	soybean methyl ester
T	temperature in the cylinder (°K)
t	time (s)
TDC	top dead centre
U	velocity of the control portion of fuel (m/s)
U_0	initial velocity of the spray at the nozzle (m/s)
U_m	velocity of the spray's front (m/s)
V	cylinder volume (m^3)
x	fraction of heat release
x_o	fraction of the fuel vapor formed during ignition delay and burnt out

Greek symbols

σ	fraction of the fuel injected into the cylinder
σ_u	fraction of the vapor formed during the ignition period
τ	ignition delay (s)
θ	crank angle (°)
ϕ	equivalence ratio
φ	function for description of the completion of combustion
γ	adiabatic exponent of exhaust gas
ξ_b	efficiency of air used

of biodiesel and petro diesel fuels. Although biodiesel does have a higher cetane number than petro diesel and therefore should improve combustion and lower NOx, other physical properties such as viscosity and bulk modulus impact the injection and combustion behavior of the fuels as well. Biodiesel has a higher bulk modulus than conventional petro diesel, which has been shown to contribute to higher NOx production. It is well known that the advancement of injection timing will increase NOx emissions, and the fuel injection timing can be impacted by the bulk modulus, i.e., the compressibility of the fuel. The difference in compressibility between biodiesel and petro diesel fuels leads to an advance in injection timing which consequently can lead to a greater opportunity to form thermal NOx [22,23]. The dominant effect on NOx emissions was the timing of the combustion process initiated by the start of injection, and the timing of maximum heat release rate and maximum temperature [24]. Prior to the above work [25] showed that the NOx increase resulting from biodiesel fueling with certain types of injection systems is partly attributable to an inadvertent advance of fuel injection timing. These observations have been confirmed and extended by [26–28]. In the present study a computational modeling using the simulation software Diesel-rk and experiments were conducted on a diesel engine fueled with diesel, soybean methyl ester (SME) and their blends on volume basis. The simulation software was applied to evaluate optimization strategies for reducing NOx emissions from biodiesel combustion.

2. Physical properties of biodiesel

Physical properties of the fuel are necessary as input data for the calculation of the spray evolution dynamics, size of droplets and, consequently, the evaporation and heat release rates. Table 1 presents the properties of different blends of diesel fuel and soybean methyl ester.

The theoretical analysis and experimental tests were carried out on a naturally aspirated, air cooled, single cylinder, direct injection diesel engine. The specifications of the engine are shown in Table 2.

3. Theoretical analysis

The software Diesel-rk is intended for the calculation and optimization of internal combustion engines. It has advanced RK-model of mixture formation and combustion in a diesel engine, and also the tool for multiparameter optimization. In the multizone com-

Table 1
Properties of diesel fuel and various blends of SME [29].

Property	Diesel	B20% SME	B40% SME	SME
Chemical formula	$C_{13.77}H_{23.44}$	$C_{14.97}H_{26.33}O_{0.34}$	$C_{16.07}H_{28.94}O_{0.68}$	$C_{19}H_{35}O_2$
Density at 15 °C(kg/m^3)	830	841	852	876
Viscosity at 40 °C (cst)	3.0	3.34	3.68	4.25
Calorific value (MJ/kg)	42.5	41.18	39.89	36.22
Flash point (°C)	76	86.8	97.6	130
Cetane number	48	48.69	49.37	51.3

Table 2
Specification of engine.

Engine make	Kirloskar TAF-1
Engine type	4-Stroke, Diesel engine
Number of cylinder	1
Bore × stroke	87.5 × 110 mm
Cylinder capacity	0.66 L
Compression ratio	17.5
Rated power	4.4 kW, 1500 rpm
Orifice diameter	0.15 mm
Injection pressure	220 bar

Author's personal copy

bustion model, the spray is split into seven characteristic zones, as shown in Fig. 1. In each zone specific evaporation and burning conditions are specified in the model. The spray evolution passes through three stages: (1) Initial formation of dense axial flow. (2) Main stage of cumulative spray evolution. (3) Period of spray interaction with the combustion chamber walls and fuel distribution on the walls. The border between the initial and main stages of spray evolution corresponds to the moment when the axial flow close to the spray tip starts to deform and break up, forming a condensed mushroom-shaped forward front.

As the spray moves on, constant breakup of the spray forward part takes place and the front is renewed by new flying fuel portions. The delayed droplets move from the breaking front to the environment. The moving spray carries the surrounding gas with it. The gas velocity in the environment being rather low, meanwhile gas in the axial core is rapidly accelerated to the velocity close to that of droplets. The core diameter in the cross section is about 0.3 of the spray outside diameter. The current position and the velocity of an elementary fuel mass (EFM) injected during small time step and moving from the injector to the spray tip are related as:

$$\left(\frac{U}{U_o}\right)^{3/2} = 1 - \frac{l}{l_m} \tag{1}$$

As an illustration, Fig. 2 presents the variation of spray evolution parameters as functions of time. The general principle evaporating equations are mentioned in [30]. Same operating conditions and fuel properties with engine specifications were used as input data to the software.

3.1. Heat release model

When calculating the heat release in the cycle, the combustion process of the fuel is split, as usual, into four stages, having unique physical and chemical features which limit the speed of the burning. These are as follows:

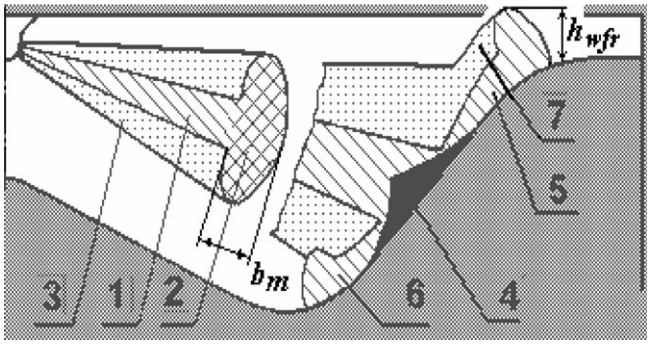

Fig. 1. Characteristic zones of the diesel spray.

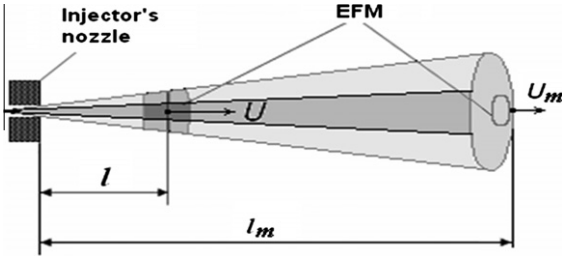

Fig. 2. Variation of spray evolution with time.

(a) Ignition delay period.

The auto ignition delay period is calculated by modified Tolstov's equation:

$$\tau = 3.8 * 10^{-6}(1 - 1.6 \times 10^{-4} \cdot n)\sqrt{\frac{T}{P}} \cdot \exp\left(\frac{E_a}{8.312T} - \frac{70}{CN + 25}\right) \tag{2}$$

(b) Premixed combustion phase.

During premixed combustion phase the heat release rate is given by:

$$\frac{dx}{dt} = \varphi_o(A_o(m_f/V_i).(\sigma_{ud} - x_o) \cdot (0.1\sigma_{ud} + x_o)) + \varphi_1(d\sigma_u/dt) \tag{3}$$

(c) Mixing controlled combustion phase.

In the mixing controlled combustion period the heat release rate can be determined as;

$$\frac{dx}{dt} = \varphi_1(d\sigma_u/dt) + \varphi_2(A_2(m_f/V) \cdot (\sigma_u - x)(\phi - x)) \tag{4}$$

(d) Late combustion phase. In this phase the heat release rate is:

$$\frac{dx}{dt} = \varphi_3 A_3 K_T(1 - x)(\xi_b \cdot \phi - x) \tag{5}$$

In these equations it is assumed that $\varphi_o = \varphi_1 = \varphi_2 = \varphi$ which is function describing completeness of fuel vapor combustion in the zones. During the simulation process the heat transfer in the cylinder is taken into account and heat transfer coefficients for its different zones are calculated using [31].

3.2. Modeling of NOx formation

While nitric oxide (NO) and nitrogen dioxide (NO_2), are usually grouped together as (NOx) emissions. NO is predominant in diesel engine. Therefore; only NO formation is considered and all calculations are carried out with thermal mechanism. Features of the designed procedure are:

1. Step by step calculation of equilibrium composition of combustion products for eighteen species in the burnt gas zone.
2. Kinetic calculation of thermal nitrogen oxides formation with chain Zeldovich mechanism.

One of the basic reactions of nitrogen oxide is:

$$N + O_2 \leftrightarrow NO + O \tag{6}$$

The rate of this reaction (Eq. (6)) depends on concentration of atomic oxygen. The volume concentration of NO in combustion products formed in a current calculation step is defined with equation

$$\frac{d[NO]}{d\theta} = \frac{2.33 * 10^7 p.e^{-\frac{38020}{T_Z}}[N_2]_e[O]_e(1 - ([NO]/[NO]_e)^2)}{RT_Z(1 + (2365/T_Z) \cdot e^{\frac{3365}{T_Z}} \cdot [NO]/[O_2]_e)} \cdot \left(\frac{1}{rps}\right) \tag{7}$$

3.3. Modeling of soot concentration

Soot is a fine dispersion of black carbon particles in a vapor carrier. The main source of soot is from the incomplete hydrocarbon combustion. Soot particles form, grow, and oxidize as a result of chemical reactions that occur during combustion. Exhaust soot concentration related to normal conditions are as follows:

Author's personal copy

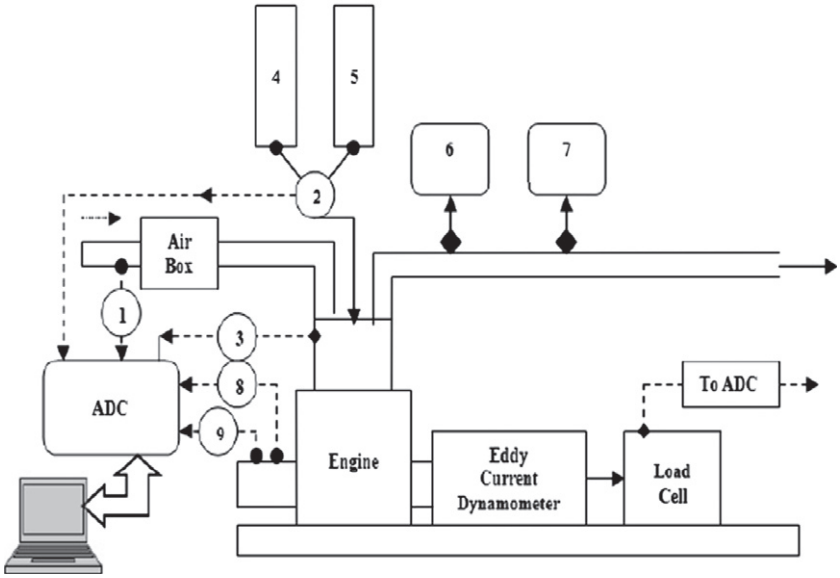

1. Air flow sensor 2. Fuel flow sensor 3. Pressure sensor
4. Diesel tank 5. Biodiesel tank 6. Five gas analyze r
7. Smoke meter 8. Speed meter 9.Crank angle encoder.

Fig. 3. Schematic diagram of the experimental setup.

$$[C]_H = \int_{\theta_B}^{480} \frac{d[C]}{dt} \cdot \frac{d\theta}{6n} \left(\frac{0.1}{p}\right)^{\gamma} \quad (8)$$

The Hartidge smoke level is calculated from the following equation;

$$\text{Hartidge} = 100[1 - 0.9545.\exp(-2.4226[C])] \quad (9)$$

An experimental curve was used to calculate the Bosch smoke number (BSN) as a function of Hartidge equation. Particulate matter emission is calculated by [32], as a function of Bosch smoke number:

$$[\text{PM}] = 565\left(\ln\frac{10}{10 - \text{Bosch}}\right)^{1.206} \quad (10)$$

Another important equation is the air pollutant emissions (SE) which is the summary of PM and NOx emissions:

$$\text{SE} = C_{\text{PM}}\left[\frac{\text{PM}}{0.15}\right] + C_{\text{NO}}\left[\frac{\text{NOx}}{7}\right] \quad (11)$$

4. Experimental test setup

The simulation results of Diesel-rk software are validated with experimental test results. The engine used in the present study was a Kirloskar TAF-1, single cylinder, air cooled, vertical and direct injection diesel engine with the specification given in Table 2. The schematic diagram of the experimental setup is shown in Fig. 3. The engine is coupled to an eddy current dynamometer. The inlet side of the engine consists of anti pulsating drum and air temperature measuring device. The exhaust side of the engine consists of exhaust gas temperature indicator, exhaust gas analyzer (AVL 437 Di Gas 444) and smoke meter (AVL-415). The operating ranges with accuracy for gas analyzer and smoke meter given in Table 3. A 64 bit DAQ system is also provided with the test rig to acquire crank angle and cylinder pressure data. The test rig is installed with AVL software for obtaining various curves and results during operation. A constant speed of 1500 rpm at variable loads with diesel as fuel was carried out to generate baseline data. Three test samples were prepared, namely B20% SME, B40% SME, and B100% SME blends by volume and similar experiments were conducted over the same range of loads. Engine was run with each biodiesel for 2 hours continuously and then the test results were obtained and compared with the baseline data. Three sets of observations were taken and the average value is considered for this study.

Table 3
Specifications of Gas analyzer (AVL 437 DiGas 444) and smoke meter (AVL 415).

Emission	Range	Accuracy
CO	0–10% vol	±0.2%
CO_2	0–20% vol	±1%
HC	0–20,000 ppm	±10 ppm
O_2	0–22% vol	±0.2%
NOx	0–5000 ppm	±10 ppm
Opacity	0–100%	±1%

5. Results and discussion

5.1. Combustion analysis

5.1.1. Cylinder pressure

In a diesel engine the cylinder pressure depends on the fuel burning rate during the premixed burning phase and higher cylinder pressure ensures better combustion and heat release. Fig. 4 shows the variation of cylinder pressure with crank angle at full load for diesel and SME blends. It can be seen that cylinder pressure for soybean biodiesel (B100%) is lower than that of diesel by 2.5% due to the reduction in the heat supply for the blended fuel. It is noted that the maximum pressure obtained for biodiesel is closer to TDC than diesel fuel. The cylinder pressure trend of B20% SME is found close to that of pure diesel operation. The simulation results are verified with the experimental results at the same operating conditions.

5.1.2. Cylinder temperature

The predicted overall cylinder temperature is shown in Fig. 5. Higher cylinder temperatures were observed for SME blends com-

Author's personal copy

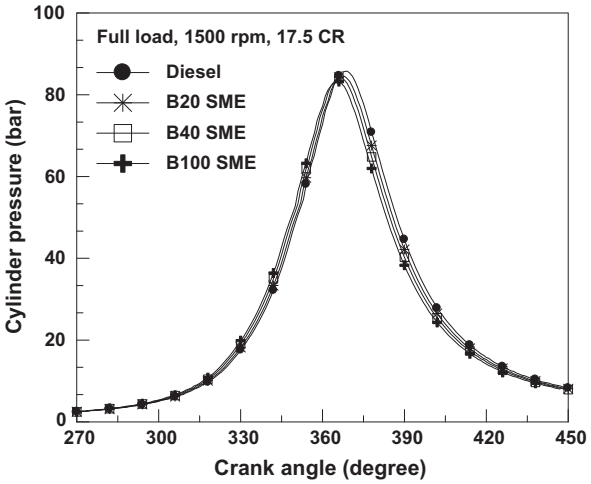

Fig. 4. Variation of cylinder pressure with crank angle.

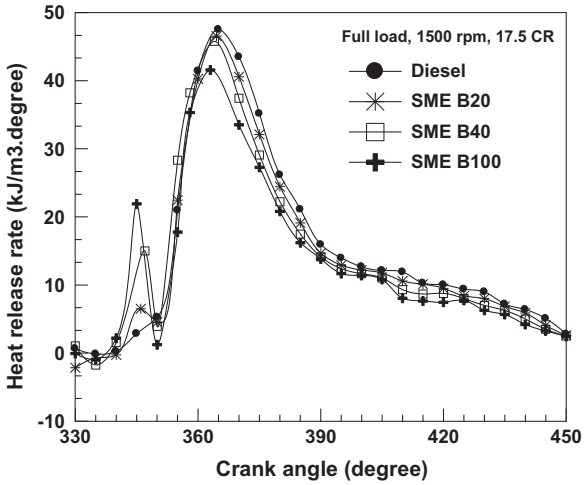

Fig. 6. Variation of heat release with crank angle.

pared to diesel fuel. The higher overall temperature is an indicator of higher flame temperatures which will cause higher NOx emission. The maximum difference in temperature between SME and diesel was 85 °K. The higher cylinder temperature was the direct reason for higher NOx emission from SME biodiesel.

5.1.3. Heat release rate

Fig. 6 presents the computed heat release rate for diesel fuel and SME biodiesel. It is evident from this figure that all biodiesel blends had earlier start of combustion, but slower combustion rate. The earlier start of combustion was caused by the advancement in the injection timing and the slower premixed combustion rate due to less energy released in premixed phase. In the diffusion combustion phase, the SME biodiesel fuel had rapid combustion because at this phase most of fuel gets vaporized and burned [19].

5.2. Performance and emission analysis

5.2.1. Brake thermal efficiency and brake specific fuel consumption

Brake thermal efficiency (BTE) is one of the main important performance parameters which indicate the percentage of energy present in the fuel that is converted into useful work. Fig. 7 presents the variation of BTE with SME biodiesel blends. In the Diesel-rk results it is observed that BTE of soybean blends were lower than that of pure diesel for the entire load by 7% while it was 8.07% in the experimental results (Table 6 for more details), both experimental and Diesel-rk results have same behavior with small difference. The decreasing trend in efficiency with increase in concentration of SME in diesel may be due to lower heating value of biodiesel over the nominal diesel fuel. It also may be caused by its poor atomization due to its high viscosity. Fig. 8 presents the BSFC, which was found to increase with the increasing percentage of biodiesel in the fuel. BSFC for all SME blends is higher than diesel fuel by 17.31%, while it was recorded 14.65% in the experimental tests. The increase in BSFC is due to higher density and lower heating value, since methyl esters have heating values that are about 12.4% less than pure diesel. These results are similar to those of [33,34].

5.2.2. Bosch smoke number and NOx emissions

Fig. 9 explains the relation between the Bosch smoke number (BSN) with different percentage of SME blending theoretically and experimentally. The smoke levels for all SME percentages are lower than that of diesel. Based on the Diesel-rk results, the average smoke level for B20, B40, and B100 were less than that of diesel fuel by 25.27%, 36.93%, and 52.96% respectively. This is because smoke decreases with high oxygen content in the biofuel that con-

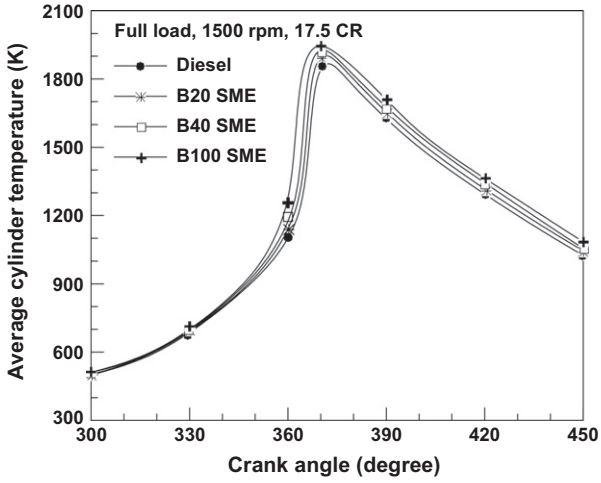

Fig. 5. Variation of average cylinder temperature with crank angle.

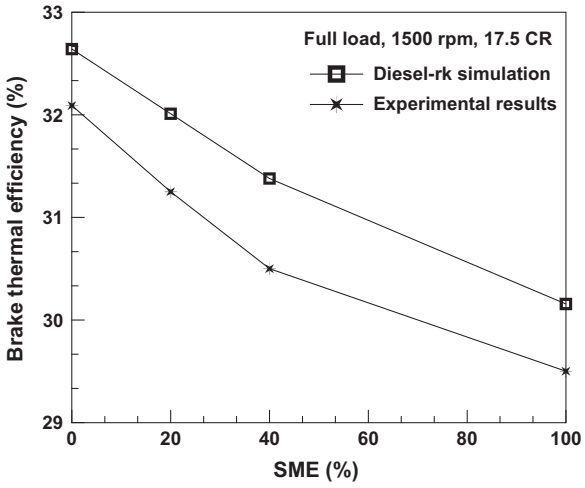

Fig. 7. Variation of BTE with SME blending.

Author's personal copy

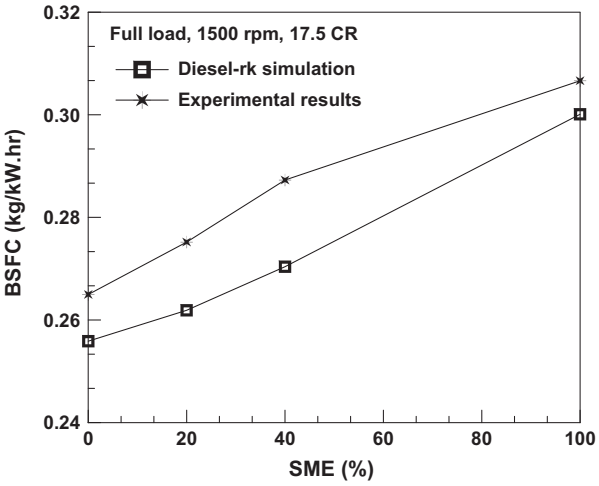

Fig. 8. Variation of BSFC with SME blending.

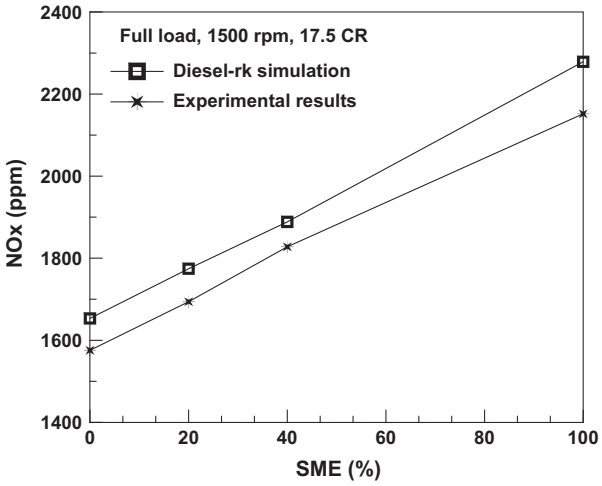

Fig. 10. Variation of NOx with SME blending.

tributes to complete fuel oxidation even in locally rich zones, so the oxygen within the fuel decrease the tendency of a fuel to produce soot [26]. Another reason for smoke reduction when using biodiesel is the lower C/H ratio as compared to pure diesel fuel. Fig. 9 shows the NOx emissions which are higher for all blending of SME than that of pure diesel fuel. According to the experimental results there is 35.1% increase in the NOx emission as a result of increasing the percentage of SME from (0–100)% with slight difference from Diesel-rk software results (Table 6). However, the NOx emissions for B20% are higher than that of base line diesel operation by 7.33%. This is associated with the oxygen content in the biodiesel hence the fuel oxygen may provide additional oxygen for NOx formation. It is well known that NOx emissions are related to start of combustion timing and the energy released in premixed burning. Earlier start of combustion causes higher cylinder pressure and higher combustion temperature, [35] (see Fig. 10).

5.2.3. Particulate matter and Summary of PM and NOx emissions

The empirical equation for the emissions of PM and NOx (Eq. (11)) is computed for different percentages of SME biodiesel. Fig. 11 presents the effect of SME blending on the PM and SE emissions. There is an increase in SE emissions by 4.45% with B20 SME as compared with pure diesel fuel. It can be seen from Fig. 11 that the level of PM for SME blending are less than that of diesel fuel. There is a reduction in the emissions of PM by 32.93%, 45.153%, and 59.63% for B20%, B40%, and B100% respectively as compared to conventional diesel fuel.

5.3. Optimization strategies

For diesel engines, smoke and NOx are the typical problematic pollutants. In conventional diesel combustion, these pollutants are particularly difficult to manage due to a soot-NOx tradeoff, whereby reduction of one pollutant generally results in an increase of the other. As a result, engine companies typically rely on after treatment systems in order to meet emission regulations for soot and NOx. This section deals with one dimensional strategy, 2-dimensional strategy and multidimensional optimization technique to reduce both NOx and smoke emissions from diesel engine working on B20% SME, at constant speed 1500 rpm.

5.3.1. One dimensional strategy

5.3.1.1. Cooling air temperature. The effect of variable intake air temperature on the emissions of NOx, SE and BSN, in addition to BSFC as a performance parameter has been studied. It is observed that cooling air temperature from (55–15) °C lead to reduction in NOx, air pollutant emissions (SE), Bosch smoke number and BSFC by 10.53%, 17.63%, 24.35%, and 6.2% respectively as compared to base line operation, because reduced intake air temperature can decrease combustion temperature, which consequently suppresses NOx emissions.

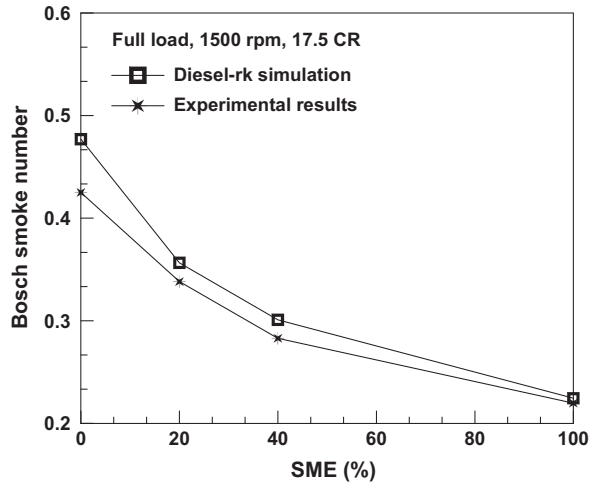

Fig. 9. Variation of BSN with SME blending.

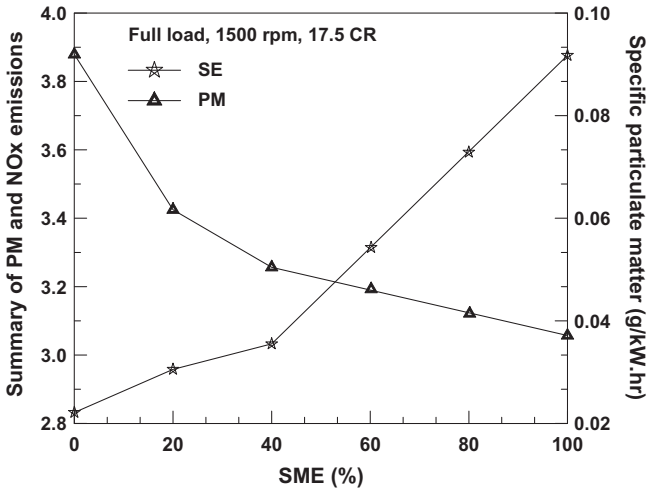

Fig. 11. Variation of SE and PM emissions with SME blending.

Author's personal copy

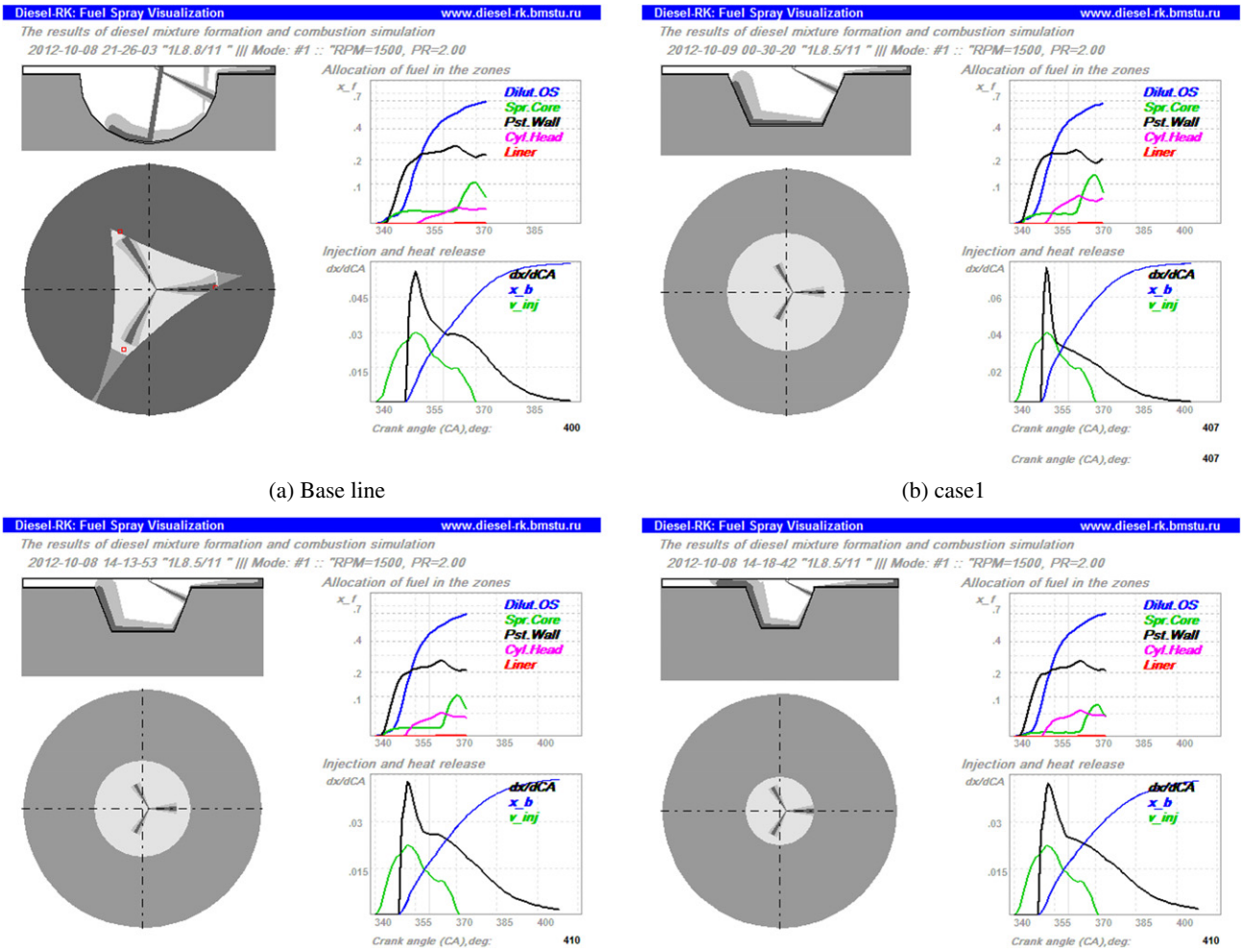

Fig. 12. (a–d) Simulation results of different diameter and depth of piston bowl configurations on the allocation of fuel in the zones and heat release diagram compared with the baseline operation.

Table 4
Simulation results of piston bowl design.

Case	Bowl diameter (mm)	Bowl depth (mm)	NOx (ppm)	SE (g/kW/h)	BSFC (kg/kW h)
Base	line	47	23.2	1784.3	2.9563
	0.26090	Case 1	40	25	1367.7
	2.1959	0.26192			
Case 2	35	30	1305.3	2.2161	0.26121
Case 3	25	32	1261.7	2.3468	0.26267
Case 4	20	35	1248.0	2.3990	0.26370

5.3.1.2. Retarding injection timing. The computational model indicates that retarding the injection timing from (27–17) °CA BTDC reduces NOx, SE and BSFC by 42.85%, 39.28%, 8.9% respectively while increases the smoke level sharply.

5.3.1.3. Piston bowel design. Fig. 12 explains the effect of piston bowl design on the performance and emissions of B20% SME. According to the main dimensions, the depth and diameter of piston bowl are changed in four cases and compared with the base line. From the simulation result of the Diesel-rk software it is found that deeper bowel with small diameter gives a good reduction in the NOx and SE emissions; the opposite behavior was noticed for good reduction in BSN. The computed results are listed in Table 4.

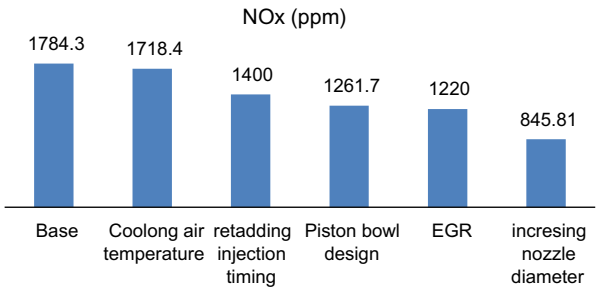

Fig. 13. Comparison of predicted NOx with different strategies.

The case no. 3 is chosen as the best one as its gives good reduction in the NOx & SE emissions by 18.14% and 27% respectively while keeping BSFC at the same level.

5.3.1.4. Exhaust gas recirculation ratio. It can be noticed that increasing exhaust gas recirculation ratio (EGR) from (0–0.06) causes a reduction in the NOx and SE emissions by 31.62%, 27.65% respectively. One possible explanation is that for biodiesel, more oxygen existed in the exhaust gas; therefore, less air was

Author's personal copy

Table 5
Computed results for the Scanning 2D simulation.

Case	EGR: CR	NOx (ppm)	SE (g/kW h)	BSN	BSFC $*10^{-2}$ (kg/kW h)	Reduction in NOx (%)	Reduction in SE (%)	Reduction in BSN (%)	Increase BSFC (%)
Base	0: 17.50	1784.30	2.95	0.35	26.08	0	0	0	0
Case1	0.06: 15	1007.20	1.79	0.41	26.54	43.55	39.4	17.40	1.75
Case2	0.04: 16	1482.40	2.50	0.39	26.18	16.91	15.14	11.10	0.36
Case3	0.04: 19	1569	2.65	0.32	27.10	10.04	10.34	10.02	3.90
Case4	0.06: 19	1376.20	2.36	0.32	27.43	22.87	20.2	8.13	5.14

Table 6
Comparison of experimental results with Diesel-rk software results.

% Change in parameter	Biodiesel blending (0–100)%	Experimental results (%)	Diesel-rk software results (%)	Δ (%)
Peak pressure	From 0 to 100	2.98	2.50	0.59
IMEP	From 0 to 100	5.08	4.48	0.60
BTE	From 0 to 100	8.07	7.00	1.07
BSFC	From 0 to 100	14.65	17.31	2.66
Smoke	From 0 to 100	48.31	52.96	4.64
NOx	From 0 to 100	35.10	38.43	3.33

needed that reduced the N_2 intake into the engine cylinder, which consequently reduced NOx emissions.

5.3.1.5. Nozzle diameter. It is observed that increasing nozzle diameter from 0.1 to 0.25 mm causes reduction in the NOx up to 54.34%, but at the same time causes increase in the emissions of SE and BSN. The increase in the nozzle diameter produces a decrease in the injection pressure that leads to less depth of jet penetration which decreases the combustion temperature and hence reduced NOx formation. On the other hand smaller diameter of nozzle causes increase in the pressure of injection and lead to faster evaporation and mixing and higher heat release rate due to faster combustion. This effect explains the higher NOx obtained with smaller nozzle diameter. The same results were represented by [36]. Fig. 13 shows the summary comparison of predicted NOx with all strategies used in this paper in bar chart, it is found that most reduction in NOx was in retarding injection timing and increasing nozzle diameter as compared to other strategies. One of the drawbacks of the one dimensional search is the decreasing of a level of NOx emission is accompanied by considerable increase in the smoke emission and fuel consumption except cooling air temperature strategy.

5.3.2. Two dimensional scanning strategy

The research of optimum combination of compression ratio and EGR was made by scanning 2D method. The compression ratio is changed from (15–19) and the exhaust gas recirculation ratio changed from (0–0.06). The following are some of the simulation results listed in Table 5. These cases are chosen from the simulation results as they give best matched results including good reduction in emissions as compared to base level emissions, with slight increase in the BSFC. The case no. 4 is chosen as the best one as its gives good reduction in all emissions of biodiesel with a reasonable increase in the BSFC.

5.3.3. Multidimensional optimization strategy

In concern with the results obtained in the simulation of scan 2D for case 4, there is still an increase in the BSFC. A multidimensional optimization strategy using Rosenbrok method is used which aims to find out the optimum combination between compression ratio, injection timing, EGR, nozzle diameter, and swirl ratio, so as to reach the lowest reduction in the emissions of B20% SME with the lowest level of BSFC. This is clearly shown in bar charts of Figs. 14 and 15 for the comparison of predicted SE, and BSFC respectively. The details of the Rosenbrok method of optimization used are explained with all the limiting parameters, and optimized parameters in [37]. The goal function (Eq. (11)) is a function of five variables (CR, Nozzle diameter, Injection timing, Swirl ratio, and EGR). It is observed that best choice for the optimization gives 43.4% reduction in the SE emissions and 50.26% reduction in the NOx emission compared to base line operation of B20 SME at 16 CR, 0.15 mm nozzle diameter, 17 CA° BTDC injection timing, 1.5 swirl ratio, and 0.06 EGR.

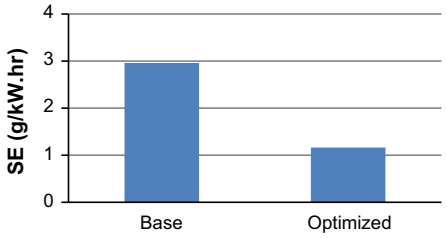

Fig. 14. Comparison of optimized SE in optimization strategy.

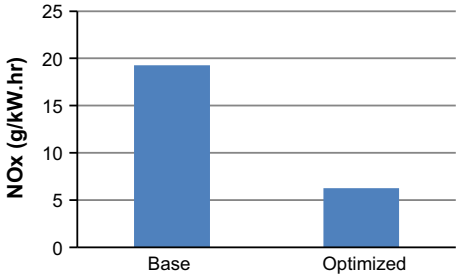

Fig. 15. Comparison of optimized NOx in optimization strategy.

5.4. Model verification

All the combustion, performance and emission parameters obtained from Diesel-rk software are compared with the experimental results of full load with the same range of operating conditions. The difference between these results is reported and arranged in Table 6.

6. Conclusions

The following conclusions can be drawn from this study.

1. The peak pressure was observed to be closer to TDC when blending of SME increased.
2. All blends of SME had earlier start of combustion as compared to base line diesel due to the shorter ignition delay which is influenced by cetane number.

Author's personal copy

3. Increasing the percentage of SME was noticed to reduce the brake thermal efficiency slightly and increase the BSFC.
4. A good reduction in the Bosch smoke number and PM emission for all blends of SME relative to that of diesel fuel.
5. All blends of SME are observed to emit higher NOx emission compared to the nominal diesel fuel
6. The best blending ratio is B20% SME which gives same performance results, good reduction in the emissions and less increase in the NOx emissions as compared with B40% & B100% SME biodiesel respectively.
7. All the one dimensional search strategies are found to reduce one emission and increase another, except cooling air temperature is able to reduce the NOx with BSN and BSFC simultaneously.
8. Increasing the EGR with CR in the scan 2D strategy is observed to give reduction in the SE, NOx, and BSN respectively with slightly increase in BSFC.
9. Using the multidimensional optimization gives 50.26% reduction in the NOx and 43.4% reduction in the SE emissions compared to base level of B20 SME.

References

[1] Yoon S, Lee C. Experimental investigation on the combustion and exhaust emission characteristics of biogas–biodiesel dual-fuel combustion in a CI engine. J Fuel Process Technol 2011;92:992–1000.
[2] Kim MY, Yoon SH, Hwang JW, Lee CS. Characteristics of particulate emissions of compression ignition engine fueled with biodiesel derived from soybean. J Eng Gas Turbine Power 2008;130:1–7.
[3] Oner C, Altun S. Biodiesel production from inedible animal tallow and an experimental investigation of its use as alternative fuel in a direct injection diesel engine. J Appl Energy 2009;86:2114–20.
[4] Roberto G, Oscar E, Valdir D, Dalni MM, Ednilton T. Use of soybean oil in energy generation. Recent Trends Enhancing Divers Qual Soybean Prod 2011:15–7.
[5] Zhang X, Gao G, Li L, Wu Z. Characteristics of combustion and emissions in a DI engine fueled with biodiesel blends from soybean oil, SAE 2008-01-1832.
[6] Labeckas G, Slavinskas S. The effect of rapeseed oil methyl ester on direct injection diesel engine performance and exhaust emissions. J Energy Convers Manage 2006;47:1954–67.
[7] Labeckas G, Slavinskas S. Performance and emission characteristics of a direct injection diesel engine operating on KDV synthetic diesel fuel. J Energy Convers Manage 2013;66:173–88.
[8] Canakci M. Performance and emissions characteristics of biodiesel from soybean oil. Proc Inst Mech Eng Part D: J. Automob Eng 2005;219:915–22.
[9] Ushakov S, Valland H. Combustion and emissions characteristics of fish oil fuel in a heavy-duty diesel engine. J Energy Convers Manage 2013;65:228–38.
[10] Scholl K, Sorenson S. Combustion of soybean oil methyl ester in a direct injection diesel engine, SAE 930934; 1993.
[11] Rakopoulos CD, Antonopoulos KA, Rakopoulos DC. Development and application of multi-zone model for combustion and pollutants formation in direct injection diesel engine running with vegetable oil or its bio-diesel. J Energy Convers Manage 2007;48:1881–901.
[12] Buyukkaya E. Effects of biodiesel on a DI diesel engine performance, emission and combustion characteristics. J Fuel 2010;89:3099–105.
[13] Hamdan MA, Haj Khalil R. Simulation of compression engine powered by biofuels. J Energy Convers Manage 2010;51:1714–8.
[14] Masood M, Mehdi SN, Reddy P. Experimental investigations on a hydrogen–diesel dual fuel engine at different compression ratios. J Eng Gas Turbine Power 2007;129:572–8.
[15] Qi DH, Chen H, Geng LM, Bian YZH. Experimental studies on the combustion characteristics and performance of a direct injection engine fueled with biodiesel/diesel blends. J Energy Convers Manage 2010;51:2985–92.
[16] Rakopoulos CD, Antonopoulos KA, Rakopoulos DC, Hountalas DT. Multi-zone modeling of combustion and emissions formation in DI diesel engine operating on ethanol–diesel fuel blends. J Energy Convers Manage 2008;49:625–43.
[17] Gumus M, Kasifoglu S. Performance and emission evaluation of a compression ignition engine using a biodiesel (apricot seed kernel oil methyl ester) and its blends with diesel fuel. J Biomass Bioenergy 2010;34:134–9.
[18] Kannan D, Pachamuthu S, Nurun Md, Hustad JE, Lovas T. Theoretical and experimental investigation of diesel engine performance, combustion and emissions analysis fuelled with the blends of ethanol, diesel and jatropha methyl ester. J Energy Convers Manage 2012;53:322–31.
[19] Yuan W. Computational modeling of NOx emissions from biodiesel combustion based on accurate fuel properties, PhD thesis, Pennsylvania Avenue, Urbana; 2005.
[20] Rakopoulos CD, Hountalas DT, Giakoumis EG, Andritsakis EC. Performance and emissions of bus engine using blends of diesel fuel with bio-diesel of sunflower or cottonseed oils derived from Greek feedstock. J. Fuel 2008;87:147–57.
[21] Gokalp B, Buyukkaya E, Soyhan HS. Performance and emissions of a diesel tractor engine fueled with marine diesel and soybean methyl ester. J Biomass Bioenergy 2011;35:3575–83.
[22] Melissa Hess A, Michael Haas J, Foglia AT. Attempts to reduce NOx exhaust emissions by using reformulated biodiesel. J Fuel Process Technol 2007;88:693–9.
[23] Tat M, Gerpen V, Soylu S, Canakci M, Monyem A, Wormley S. The speed of sound and isentropic bulk modulus of biodiesel at 21 °C from atmospheric pressure to 35 MPa. JACS 2000;77:285–9.
[24] Agarwal D, Sinha S, Kumar A. Experimental investigation of control of NO_x emissions in biodiesel-fueled compression ignition engine. J Renew Energy 2006;31:2356–69.
[25] Lei Zh, Cheung C, Zhanga WG. Influence of methanol–biodiesel blends on the particulate emissions of a direct injection diesel engine. J Aerosol Sci Technol 2010;44:362–9.
[26] Bryan Moser R, Williams A, Michael Haas J, Robert McCormick L. Exhaust emissions and fuel properties of partially hydrogenated soybean oil methyl esters blended with ultra low sulfur diesel fuel. J Fuel Process Technol 2009;90:1122–8.
[27] Mueller J, Boehman AL. An experimental investigation of the origin of increased NO_x emissions when fueling a heavy-duty compression-ignition engine with soy biodiesel. J SAE 2009:1792.
[28] Graboski M, McCormick R. Combustion of fat and vegetable oil derived fuels in diesel engines. J Prog Energy Combust Sci 1998;24:125–64.
[29] Kuleshov A, Mahkamov K. Multi-zone diesel fuel spray combustion model for the simulation of a diesel engine running on biofuel. Proc Inst Mech Eng, Part A: J Automob Eng 2007;222:309–21.
[30] Kuleshov AS. Model for predicting air-fuel mixing, combustion and emissions in DI diesel engines over whole operating range, J. SAE 2005-01-2119.
[31] Woschni G. A universally applicable equation for the instantaneous heat transfer coefficient in the internal combustion engine, SAE 670931; 1967.
[32] Alkidas AC. Relationship between smoke measurements and particular measurements, J. SAE 840412; 1984.
[33] Canakci M, Van Gerpen Jon H. Comparison of engine performance and emissions for petroleum diesel fuel, yellow grease biodiesel, and soybean oil biodiesel. In: ASAE annual international meeting sacramento convention center Sacramento, California, USA, July 30–August 1; 2001.
[34] Monyem A. The effect of biodiesel oxidation on engine performance and emissions. Ph.D. Dissertation, Department of Mechanical Engineering, Iowa State University, Ames, IA; 1998.
[35] Ozsezen AN, Canakci M. Determination of performance and combustion characteristics of a diesel engine fueled with canola and waste palm oil methyl esters. J Energy Convers Manage 2011;52:108–16.
[36] Fi Millo, Delnere D. Analysis on the effect of compression ratio, injection timing, injector nozzle holes size and number on the performance and emissions. In: GT-Suit users international conference Frankfurt, 9th October; 2006.
[37] Kuleshov AS. Use of multi-zone di diesel spray combustion model for simulation and optimization of performance and emissions of engines with multiple injection. J. SAE 2006-01-13.